Immune response and stromal changes in ductal carcinoma in situ of the breast are subtype dependent

Marie Colombe Agahozo[1] · Pieter J. Westenend[2] · Mieke R. van Bockstal [1,3] · Tim Hansum[1] · Jenny Giang[1] · Sanneke E. Matlung[1] · Carolien H. M. van Deurzen[1]

Abstract

Ductal carcinoma in situ (DCIS) associated stromal changes and influx of immune cells might be mediators of progression to invasive breast cancer. We studied the interaction between DCIS-associated stromal changes, and immune cell distribution and composition in a well-characterized patient cohort. We included 472 patients with DCIS. The presence of stromal changes, signs of regression, and DCIS-associated immune cell position were determined on hematoxylin and eosin-stained slides. Immune cell composition was characterized by immunohistochemistry (CD4, CD8, CD20, CD68, and FOXP3). The number of intraductal immune cells was quantified per mm^2. The interaction between stromal changes, signs of DCIS regression, immune cell composition and location was explored. Stromal changes and signs of DCIS regression were identified in 30 and 7% of the patients, respectively. Intraductal immune cells mainly comprised CD68+ macrophages and CD8+ T cells. Patients with stromal changes had significantly less influx of immune cells within the duct. DCIS regression was associated with an increased number of intraductal FOXP3+ T cells. The highest number of intraductal CD8+ T cells was seen in the ER+ HER2+ subtype. We suggest that DCIS-associated stromal changes prevent the interaction between immune cells and DCIS cells. However, in case of DCIS regression, we surmise a direct interaction between DCIS cells and immune cells, in particular FOXP3+ cells. Furthermore, the increased number of intraductal CD8+ T cells in the ER+ HER2+ DCIS subtype suggests a subtype-specific immune response, which is likely to play a role in the distinct biological behavior of different DCIS subtypes.

Background

Ductal carcinoma in situ (DCIS) is considered to be a non-obligate precursor of invasive breast cancer and it is treated as such, with respect to local therapy [1, 2]. DCIS is a heterogeneous disease and, similar to invasive breast cancer, it can be classified into several surrogate subtypes based on estrogen receptor (ER), progesterone receptor (PR) and human epidermal growth factor receptor (HER2) expression

as determined by immunohistochemistry [3]. Data are limited regarding the treatment-naive behavior of DCIS, but DCIS subtypes have been reported to be associated with distinct biological behavior [4, 5]. A substantial proportion of DCIS cases are associated with changes in their microenvironment, such as stromal changes and influx of immune cells [6, 7]. These changes could be important mediators of the propensity of DCIS to evolve to invasive breast cancer.

Generally, high numbers of tumor-infiltrating lymphocytes (TILs) are observed in high grade, triple negative, or HER2+ DCIS [4, 8–10]. These DCIS-associated TILs are generally located in the stroma and mainly consist of CD4+ T cells [4, 11–13]. Specific immune cell subsets are reported in association with outcome. High amounts of CD19/CD20+ B cells were associated with shorter recurrence-free survival in patients with DCIS, while high levels of CD8+ T cells were associated with a low risk for ipsilateral recurrence [11, 14, 15]. Stromal changes have also been associated with outcome and can be described as myxoid stroma or sclerotic stroma [7, 13, 15]. The presence of myxoid stroma has been associated with an increased

✉ Marie Colombe Agahozo
m.agahozo@erasmusmc.nl

1   Department of Pathology, Erasmus MC Cancer Institute, Rotterdam, The Netherlands

2   Laboratory for Pathology Dordrecht, Dordrecht, The Netherlands

3   Cliniques universitaires Saint-Luc, Brussels, Belgium

ipsilateral recurrence risk [7]. Sclerotic stroma is regarded as part of DCIS regression [13, 15]. DCIS regression is a process whereby stromal changes indulge neoplastic cells, which are replaced by fibrosis [13, 15–17]. Signs of DCIS regression are associated with high-grade DCIS, and ER/PR-negative and HER2+ subtypes [13, 15–17].

Co-occurrence of DCIS-associated stromal changes, including DCIS regression, and influx of TILs has been described [13, 15]. Intraductal influx of CD8+ T cells in particular has been linked to DCIS regression [15]. This observation suggests that DCIS regression could be the result of a targeted immune response. However, data are limited with respect to the interaction of DCIS with the surrounding stroma and immune cells. The aim of this study was therefore to evaluate the interaction between DCIS histopathological characteristics, DCIS-associated stromal changes (including signs of regression), and immune cells (composition and location) in a large, well-documented cohort of patients.

Patients and methods

Study cohort

This retrospective study included 472 patients with a primary diagnosis of pure DCIS from a previously described cohort [4]. Briefly, these patients were diagnosed at the Erasmus Medical Center Cancer Institute Rotterdam or at the Laboratory for Pathology Dordrecht between 2000 and 2016. Clinical data and a central pathology review, including assessment of DCIS characteristics and DCIS-associated TILs, were performed as previously described by Agahozo et al. [4]. DCIS surrogate molecular subtypes were based on immunohistochemistry: ER+ PR±HER2−, ER+PR±HER2+, ER−PR−HER2+, or ER−PR−HER2− (triple negative). A 10% cutoff for ER and PR was used, according to the Dutch guidelines for hormone receptor assessment in invasive breast cancer [18]. HER2 was scored as 0, 1+, 2+, or 3+, and in situ hybridization was

performed in cases with an equivocal HER2 expression, according to the ASCO/CAP guidelines [19]. Ipsilateral recurrence was defined as a histologically confirmed in situ or invasive carcinoma ≥6 months after the initial diagnosis and treatment. The median follow-up time was 98 months, ranging from 24 to 218 months. Encoded leftover patient material was used, in accordance with the Dutch Code of Conduct of the Federation of Medical Scientific Societies [20].

DCIS-associated stromal changes and signs of regression

All hematoxylin and eosin-stained slides from this cohort ($n = 472$) were reviewed to determine the presence of DCIS-associated stromal changes, which was defined as stroma within 1.0 mm of the duct. Stromal changes were classified as absent, sclerotic, or myxoid, as illustrated in Fig. 1. Sclerotic stroma was defined as a dense, eosinophilic ring surrounding the duct, and myxoid stroma was defined as 'loose' basophilic stroma. DCIS regression was assessed in 450 patients. The remaining 22 patients were excluded because of tissue inaccessibility. DCIS regression was defined as a combination of stromal changes, mostly sclerotic, and a reduction or absence of DCIS cells, whereby microcalcification or comedonecrosis might still be present. Some examples of DCIS regression are shown in Fig. 2. This definition is comparable to stages a and b from Horii et al, stages 2 and 3 from Wassermann et al., or phases B, C, and D adapted from Morita et al. [13, 15, 17]. All cases were reviewed by two observers at the same time, using a multiheaded microscope, whereby consensus was reached in case of disagreement.

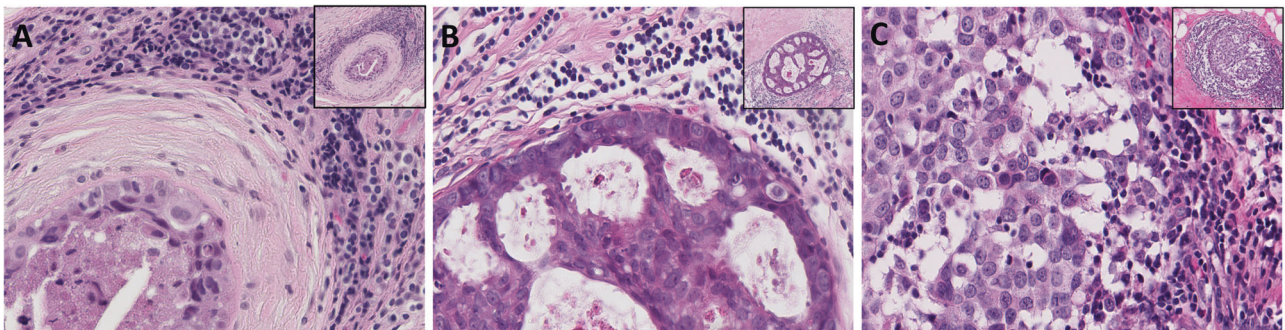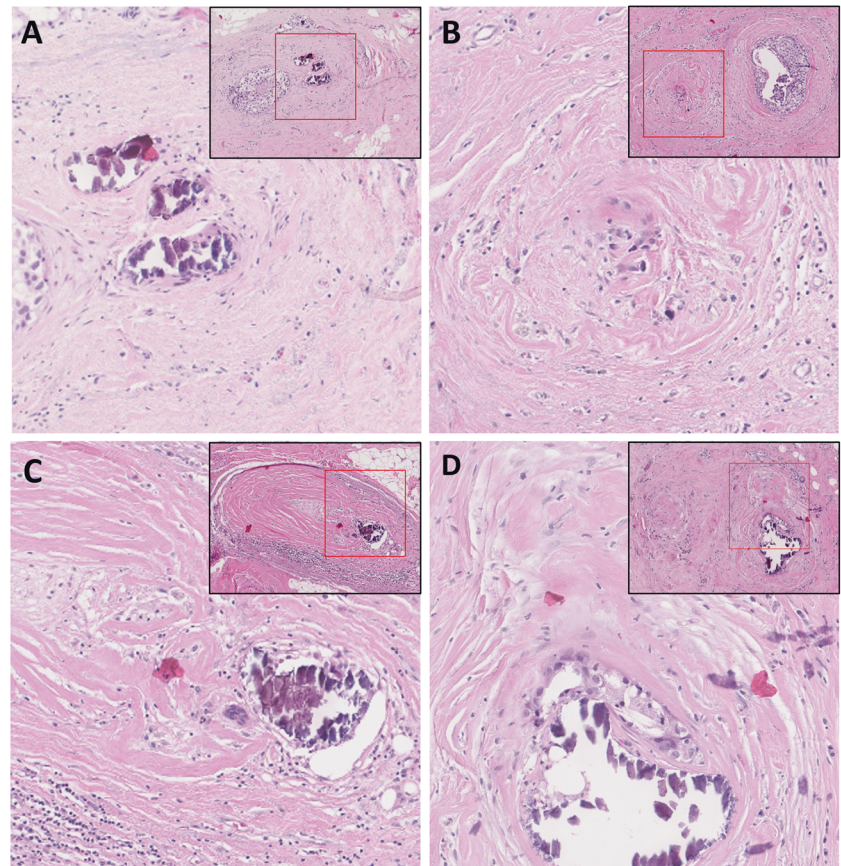### The position and composition of DCIS-associated immune cells

All cases in this cohort were previously classified as either TIL-high ($n = 131$) or TIL low ($n = 341$) based on
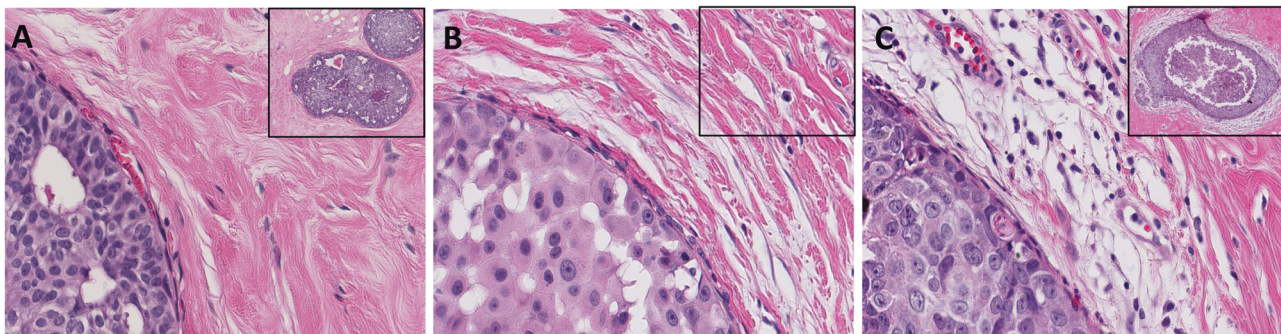
Fig. 1 Representative images of DCIS-associated stromal changes. DCIS without stromal changes **a**, DCIS with sclerotic stroma **b**, and DCIS with myxoid stroma **c**.

Fig. 2 Cases of regressive changes in DCIS. Several cases of regression, depicting 'normal' DCIS (**a**, **b**) in combination with residual calcification (**a**, **c**, **d**) and/or scare-like structures (**b**, **d**). Images are depicted at a 15× magnification, and overview images are depicted as inserts at a 5× magnification. Red boxes indicate zoomed in areas.

Fig. 3 Representative images of DCIS-associated TILs position. Representative images of periductal **a**, touching **b**, and intraductal **c** DCIS-associated TILs.

hematoxylin and eosin-stained slides. The composition of the immune cells in the DCIS-associated stroma was described previously [4]. Briefly, CD4 (T helpers), CD8 (cytotoxic T cell), CD20 (B cells), CD68 (macrophages), and FOXP3 (regulatory T cells) expressing immune cells were assessed on consecutive 4-μm thick formalin-fixed tissue slides, using the automated Ventana Benchmark ULTRA stainer (Ventana Medical System Inc.) according to the manufacturer's instructions.

For the current study, the position of the DCIS-associated immune cells was assessed for TIL-high cases based on central pathology review of hematoxylin and eosin-stained slides. The following categories were defined: intraductal (influx of immune cells within the duct), touching (immune cells in direct contact with the duct, as described by Toss et al.), and periductal (area of stroma between the duct and the immune cells) [9]. Figure 3 depicts representative images of these categories. In addition, the composition of the intraductal immune cells was determined, based on immunohistochemically stained slides. Intraductal immune cells were quantified manually by counting the number of positive cells within the duct, either within the epithelium or within the lumen, per mm^2, further described as intraepithelial or intraluminal.

Statistical analysis

IBM SPSS statistics 21.0 was used to perform the statistical analysis. The Chi-square test was used to test univariate and multivariate associations. In case of a 2×2 table, the Fisher exact test was used. A stepwise backward conditional regression model was used for multivariate testing. For variables with more than two outcome measures, we used a multinominal regression model for multivariate testing. Unpaired analysis of nonparametric continuous data was performed using the Mann–Whitney U test or the Kruskal–Wallis test for two groups and more than two groups, respectively. Analysis of paired data was performed using the Wilcoxon signed-ranks test.

Results

Stromal changes according to clinicopathological characteristics

In this cohort of 472 patients with DCIS, we observed periductal stromal changes in 143 patients (30.3%). The majority of these cases (114 out of 143; 79.7%) was classified as sclerotic and the remainder was classified as myxoid (29 out of 143; 20.3%). Baseline characteristics did not significantly differ between patients with sclerotic and myxoid stroma (Supplementary Table 1). We therefore compared patients with stromal changes to those without stromal changes in the remaining analysis.

The presence of stromal changes (either sclerotic or myxoid) was associated with several other DCIS characteristics, as depicted in Table 1. In univariate analysis, DCIS with stromal changes showed significantly more often a large size ($P < 0.0001$), high grade ($P < 0.0001$), the presence of comedonecrosis ($P < 0.0001$), ER−PR−HER2+ subtype ($P < 0.001$), and TIL-high DCIS ($P < 0.0001$). In multivariate analysis, all of these variables remained significantly associated with stromal changes, except for DCIS size and grade.

DCIS regression according to clinicopathological characteristics

We identified signs of DCIS regression in 30 out of 450 (6.7%) patients. The association between DCIS regression and DCIS characteristics is reported in Table 2. Overall, DCIS regression was associated with a larger size ($P = 0.011$), high grade ($P < 0.0001$), presence of comedonecrosis ($P = 0.013$), ER−PR−HER2+ IHC subtype ($P < 0.0001$), and TIL-high DCIS ($P = 0.006$). After multivariate analysis, only the association between DCIS regression and ER−PR−HER2+ IHC subtype remained significant ($P = 0.002$).

Immune cell position according to clinicopathological characteristics

Based on hematoxylin and eosin-stained slides, the overall TIL distribution in TIL-high cases was determined. The majority of these DCIS-associated TILs were classified as periductal (41.2%), followed by touching (35.9%) and intraductal (22.9%). Additionally, TIL position was associated with DCIS characteristics (Table 3). High-grade DCIS presented more often with periductal or touching TILs. Contrariwise, intermediate grade DCIS presented more often with influx of TILs within the ducts ($P = 0.028$). No other associations between TILs distribution and histopathological features of DCIS were observed.

For multivariate analysis, periductal TILs were set as a reference variable (Table 4). Patients with touching TILs were younger ($P = 0.013$), more likely to have a solid growth pattern ($P = 0.020$) and comedonecrosis ($P = 0.001$). Patients with intraductal TILs did not significantly differ from patients with periductal TILs.

Intraductal immune cell composition

The composition of stromal DCIS-associated immune cells in this cohort was previously described as the percentage of positive immune cells [4]. In the present study, the composition of intraductal immune cells was assessed as the number of immune cells per mm^2. Overall, the median number of intraductal immune cells per mm^2 was 11.0 (range: 0–559). The majority of these intraductal immune cells were CD68+ macrophages and CD8+ T cells followed by CD4+ T cells and CD20+ B cells, with a median (range) of 5.0 (0–63), 3.0 (0–285), 1.0 (0–83), and 0.0 (0–100) cell per mm^2, respectively. The remaining immune cells comprised FOXP3+ T cells. Intraductal immune cells were further classified as either intraepithelial or intraluminal. With regard to intraepithelial immune cells, the majority of the cells comprised CD8+ T cells. With respect to intraluminal immune cells, the majority of the cells comprised CD68+ macrophages.

Immune cell composition according to stromal changes and regression

We compared the immune cell composition according to stromal changes and signs of regression, in order to evaluate whether these changes are immune cell specific. There was no association between the periductal immune cell composition and presence of stromal changes. On the other hand, the number of intraductal CD4+, CD8+, CD20+, and CD68+ immune cells was higher in patients without stromal changes ($P = 0.011$, $P = 0.048$, $P = 0.014$, and $P = 0.003$, respectively). Specifically, a higher number of

Table 1 Clinicopathological characteristics according to DCIS-associated stromal changes.

	Periductal stromal changes (n = 472)		Univariate P-value	Multivariate P-value
	Present (n = 143) n (%)	Absent (n = 329) n (%)		
Age at diagnosis (years)			0.175	–
Median (range)	58.0 (32.0–84.0)	57.0 (27.0–84.0)		
Size (missing n = 65; cm)			**<0.0001**	0.054
Median (range)	2.90 (0.30–13.50)	1.70 (0.05–17.0)		
Growth pattern			0.282	–
Solid	81 (57)	157 (48)		
Cribriform	52 (36)	138 (42)		
Micropapillary	9 (6)	28 (9)		
Papillary	1 (1)	6 (2)		
Grade			**<0.0001**	0.066
Low	3 (2)	60 (18)		
Intermediate	27 (19)	138 (42)		
High	113 (79)	131 (40)		
Calcification			0.98	–
Absent	34 (34)	99 (30)		
Present	109 (76)	230 (70)		
Comedonecrosis			**<0.0001**	**<0.0001**
Absent	38 (27)	195 (59)		
Present	105 (73)	134 (41)		
IHC DCIS subtype (missing n = 19)			**<0.0001**	**<0.0001**
ER+PR±HER2−	36 (25)	223 (68)		
ER+PR±HER2+	30 (21)	55 (17)		
ER−PR−HER2+	55 (38)	30 (9)		
ER−PR−HER2−	15 (10)	9 (3)		
Density of TILs			**<0.0001**	0.011
Low	70 (49)	271 (82)		
High	73 (51)	58 (18)		
Ipsilateral recurence (missing n = 6)			0.162	–
No	131 (92)	319 (97)		
Yes	7 (5)	9 (3)		

Statistically significant p-values are in bold.

intraepithelial CD4+, CD8+, CD20+, and CD68+ immune cells were found in patients without stromal changes ($P = 0.014$, $P = 048$, $P = 0.002$, and $P = 0.013$, respectively). With respect to intraluminal immune cells, we observed higher numbers of CD68+ macrophages in patients without stromal changes ($P = 0.006$). Intraductal immune cell composition according to stromal changes is depicted in Fig. 4a.

Next, we compared the immune cell composition according to the presence of signs of DCIS regression. The proportion of periductal FOXP3+ T cells was higher in cases with DCIS regression compared to those without DCIS regression. We found a similar association with regard to intraductal immune cells. The number of intraductal FOXP3+ T cells was higher in case of DCIS regression ($P = 0.046$). This effect was mainly based on intraepithelial FOXP3+ T cells ($P = 0.006$). Figure 4b depicts the number of intraductal immune cells according to the presence of signs of DCIS regression.

The composition of the intraductal immune cells correlated with the DCIS surrogate molecular subtype. The ER+ PR±HER2+ subtype had the highest number of intraductal CD8+ T cells ($P = 0.020$), either intraepithelial ($P = 0.008$), or intraluminal ($P = 0.019$). The ER+PR±HER2− subtype was associated with the highest numbers of intraepithelial CD68+ macrophages ($P = 0.047$). The number of intraductal immune cells according to DCIS subtype is depicted in Fig. 5.

Table 2 The association
between DCIS regression and
clinicopathological
characteristics.

	DCIS regression ($n = 450$)		Univariate *P*-value	Multivariate *P*-value
	Yes ($n = 30$) *n* (%)	No ($n = 420$) *n* (%)		
Age at diagnosis (years)			0.469	–
Median (range)	60.5 (32.0–81.0)	58.0 (27.0–84.0)		
Size (missing $n = 61$; cm)			**0.001**	0.069
Median (range)	2.9 (2.80–3.00)	2.0 (0.10–13.5)		
Growth pattern			0.292	–
Solid	20 (67)	206 (49)		
Cribriform	8 (27)	176 (42)		
Micropapillary	2 (7)	33 (8)		
Papillary	0 (0)	5 (1)		
Grade			**<0.0001**	0.133
Low	0 (0)	58 (14)		
Intermediate	4 (13)	152 (36)		
High	26 (87)	210 (50)		
Calcification			0.835	–
Absent	9 (30)	118 (28)		
Present	21 (70)	302 (72)		
Comedonecrosis			**0.013**	–
Absent	8 (27)	215 (51)		
Present	22 (73)	205 (49)		
IHC DCIS subtype (missing $n = 18$)			**<0.0001**	**0.002**
ER+PR±HER2−	5 (17)	241 (60)		
ER+PR±HER2+	6 (20)	75 (18)		
ER−PR−HER2+	13 (43)	70 (17)		
ER−PR−HER2−	6 (20)	16 (4)		
Density of TILs			**0.006**	–
Low	15 (50)	313 (75)		
High	15 (50)	107 (25)		
Ipsilateral recurence (missing $n = 6$)			1.000	–
No	28 (97)	400 (96)		
Yes	1 (3)	15 (4)		

Statistically significant *p*-values are in bold.

Discussion

It is well known that DCIS can induce changes in its microenvironment, including periductal stromal changes and influx of immune cells, which could be mediators of DCIS behavior. However, an in-depth analysis of this interaction is still lacking. In our previous study, we described the density and composition of stromal immune cells according to DCIS subtypes [4]. In this current study, we focused on DCIS-associated stromal changes in relation to immune cell position/composition.

Overall, stromal changes were observed in 30% of all cases, which predominantly consisted of sclerotic stroma (80%). These cases were generally high grade, ER−HER2+

DCIS and associated with a high number of immune cells. Sclerotic stroma has previously only been described as part of DCIS regression in high-grade DCIS [13]. The presence of myxoid stroma has been reported to correlate with a more aggressive DCIS phenotype [7], which is in line with our data. In our study, signs of DCIS regression were detected in 7% of all patients. This proportion is consistent with an earlier study, which used a similar definition for regression [17]. Several others studies described higher rates of DCIS regression, ranging between 39 and 59% [13, 15, 16]. However, these studies included smaller cohorts and/or had a different, less stringent definition of DCIS regression. Nevertheless, we observed an association between DCIS regression and

Table 3 The association between the immune cell position and clinicopathological characteristics.

	Immune cell position (n = 131)			Univariate P-value
	Periductal (n = 54) n (%)	Touching (n = 47) n (%)	Intraductal (n = 30) n (%)	
Age at diagnosis (years)				0.073
Median (range)	60 (32–81)	56 (27–73)	53 (35–85)	
Size (missing n = 17; cm)				0.339
Median (range)	3.00 (0.10–9.00)	2.55 (0.1–9.20)	3.00 (0.30–16.00)	
Growth pattern				0.081
Solid	25 (46)	34 (72)	20 (67)	
Cribriform	22 (41)	9 (19)	6 (20)	
Micropapillary	7 (13)	3 (6)	4 (13)	
Papillary	0 (0)	1 (2)	0 (0)	
Grade				**0.028**
Low	0 (0)	1 (2)	2 (7)	
Intermediate	5 (9)	4 (9)	8 (27)	
High	49 (91)	42 (89)	20 (67)	
Calcification				0.328
Absent	9 (17)	12 (26)	9 (30)	
Present	45 (83)	35 (74)	21 (70)	
Comedonecrosis				0.087
Absent	12 (22)	18 (38)	13 (43)	
Present	42 (78)	29 (62)	17 (57)	
IHC DCIS subtype (missing n = 3)				0.786
ER+PR±HER2−	12 (23)	9 (19)	8 (28)	
ER+PR±HER2+	13 (25)	11 (23)	10 (34)	
ER−PR−HER2+	21 (40)	22 (47)	8 (28)	
ER−PR−HER2−	6 (12)	5 (10)	3 (10)	
Ipsilateral recurence (missing n = 5)				0.793
No	50 (96)	44 (96)	26 (93)	
Yes	2 (4)	2 (5)	2 (7)	

Statistically significant p-values are in bold.

Table 4 Multivariate analysis of immune cell position according to clinicopathological characteristics.

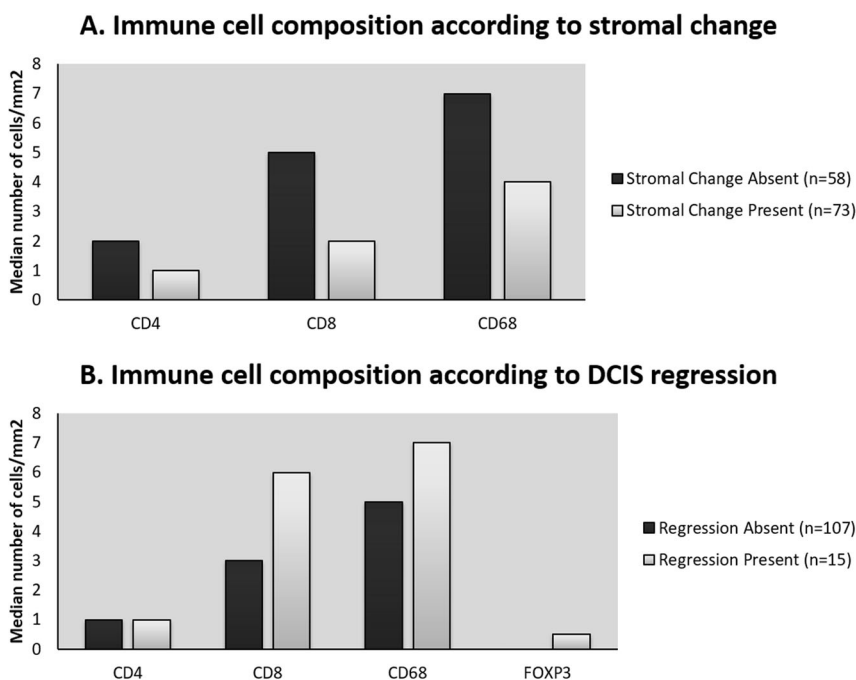|	Immune cell position (n = 131)					
	Touching* (n = 47)			Intraductal* (n = 30)		
	OR	95% CI	P-value	OR	95% CI	P-value
Age	0.96	0.93–0.99	**0.013**	0.97	0.93–1.02	0.207
Size (missing n = 17; cm)	1.05	0.92–1.20	0.472	1.17	0.99–1.39	0.067
Growth pattern	1.84	1.10–3.08	**0.020**	1.57	0.77–3.19	0.216
Grade	1.41	0.75–2.63	0.287	0.57	0.26–1.26	0.161
Calcification	0.87	0.40–1.89	0.723	0.74	0.26–2.13	0.577
Comedonecrosis	0.32	0.16–0.64	**0.001**	0.58	0.21–1.56	0.280
IHC DCIS subtype (missing n = 3)	1.05	0.75–1.47	0.776	1.29	0.80–2.09	0.300
Ipsilateral recurence (missing n = 5)	0.64	0.11–3.74	0.620	0.94	0.09–9.09	0.956

OR odds ratio.

*Periductal immune cell position set as reference variable (n = 54).

Statistically significant p-values are in bold.

Fig. 4 Intraductal immune cell composition according to DCIS-associated changes. Immune cell composition according to stromal changes **a** and DCIS regression **b**. Blue bars represent the absence of stromal change or regression, and the red bars represent the presence of stromal change or regression. The *y*-axis depicts the median number of immune cells per mm^2; the *x*-axis depicts the immune cells subset. A Mann–Whitney *U* test was used to test for differences according to stromal changes **a** or DCIS regression **b**.

A. Immune cell composition according to stromal change

Stromal Change Absent (n=58)
Stromal Change Present (n=73)

B. Immune cell composition according to DCIS regression

Regression Absent (n=107)
Regression Present (n=15)

Immune cell distribution according to DCIS subtype

CD4   CD8   CD68
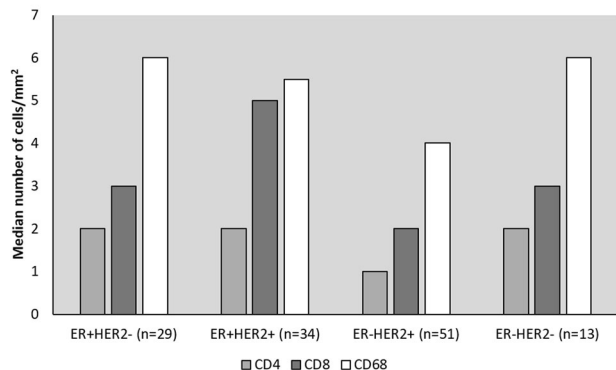
Fig. 5 Intraductal immune cell composition according to DCIS surrogate subtype. The *y*-axis depicts the median number of immune cells per mm^2; the *x*-axis depicts the DCIS surrogate subtype. A Kruskal–Wallis test was used to test for differences within DCIS groups.

HER2+ cases, which is consistent with these previously published findings.

The composition of the immune cell infiltrate differs according to its location. As previously described, DCIS-associated stromal immune cells mainly consist of CD4+ T cells [4, 11–13]. Here, we observed that intraductal immune cells predominantly comprised CD68+ macrophages and CD8+ T cells. When stratified into intraepithelial and intraluminal cells, we observed that the majority of intraepithelial cells were CD8+ T cells and that intraluminal cells mainly comprised CD68+ macrophages. These data illustrate the different biological roles of these cells, since CD8+ T cells are cytotoxic T lymphocytes that

are required to be in close proximity of the neoplastic cells, whereas CD68+ macrophages clean up necrotic cell debris and can rather be found in the lumen of the affected ducts.

Next, we observed that patients with stromal changes had significantly less influx of immune cells within the duct. These results suggest that the presence of stromal changes might act as a physical barrier for immune cells, preventing them from penetrating the basement membrane and subsequently infiltrating the ductal epithelium. This finding has been previously described by Gil Del Alcazar et al., who reported limited interaction between T cells and cancer cells, during the DCIS stage. More recently, Mitchell et al. demonstrated that focal loss of myoepithelial cells was associated with an increased number of stromal PD1+CD8+ T cells, which suggests a link between myoepithelial cells and immune surveillance [21].

Counterintuitively, we observed that DCIS regression was associated with high numbers of FOXP3+ T cells. These immunosuppressive cells are generally associated with poor outcome in advanced breast cancer and ipsilateral recurrence in DCIS [22–24]. However, in HER2+ breast cancer, they were associated with improved outcome [25, 26]. Furthermore, a recent study reported that FOXP3+ regulatory T cells opposed breast cancer progression at early stages in murine mammary tumors [27]. Additionally, a recently identified CAF-S1 subtype, which was enriched in HER2+ breast cancer, was suggested to attract and enhance T cell differentiation of C25+FOXP3+ lymphocytes [28]. We therefore hypothesize that at some stages of regression, the stroma might be more permeable, making it

accessible for T cells, specifically the FOXP3+ T cells, which might suppress progression of HER2+ DCIS.

With regard to DCIS IHC subtype, HER2-enriched DCIS is generally associated with a marked immune response [4, 8, 15]. This response could be triggered by HER2, whereby HER2 overexpression functions as an immune antigen [29]. On the other hand, HER2 overexpression increases the proliferation and growth rate of DCIS, resulting in hypoxia and increased necrosis, which might also trigger the immune response [30]. In our study, ER+HER2+ DCIS was associated with the highest numbers of intraductal CD8+ T cells. These immune cells are generally associated with improved outcome in invasive breast cancer and low risk for recurrence in DCIS [11, 26, 31]. In pure DCIS, intraductal CD8+ T cells were also associated with lower DCIS grade, absence of comedonecrosis, and a low DCIS density score based on the number of DCIS foci [11]. Overall, these results suggest that in ER+HER2+ DCIS, CD8+ T cells might mediate their indolent behavior. Our study included a large, well-characterized DCIS cohort, enabling us to study the DCIS microenvironment in detail. However, our study also had several limitations. First, treatment modalities were unknown, the number of ipsilateral recurrences was too low and the median follow-up time too short to study the association between stromal changes, and immune cell composition/position and ipsilateral recurrence risk. Secondly, we used a limited number of markers to determine the immune cell composition. The use of additional markers could provide additional information with respect to immune activation. It would therefore be interesting to compare our findings with the results of functional ex vivo assays. Thirdly, the number of triple-negative DCIS cases was limited in our cohort, which is a well-known phenomenon in DCIS series [8]. Lastly, we determined stromal changes based on hematoxylin and eosin staining, while the use of immunohistochemical markers could provide additional information regarding subtypes of cancer-associated fibroblasts. Besides, stromal architecture is a feature with substantial interobserver variability, which could have affected our findings [32].

In conclusion, our study demonstrated the association between DCIS-associated stromal changes, including signs of regression in a particular subset of DCIS, and high numbers of immune cells. We demonstrated a site-specific immune cell composition: stromal immune cells include a high proportion of CD4+ T cells, while the influx of immune cells into the duct is mainly based on CD8+ T cells and CD68+ macrophages. The influx of immune cells was significantly lower in patients with DCIS-associated stromal changes compared to those without stromal changes. This suggests that the stroma might function as a physical barrier, preventing the interaction of immune cells with DCIS cells. Signs of DCIS regression on the other hand were

associated with an increased numbers of FOXP3+ T cells within the duct, suggesting interaction with DCIS cells and an active role for FOXP3+ cells in DCIS regression. Furthermore, the increased number of CD8+ T cells in the HER2+ DCIS subtype suggests that the immune response is subtype specific. Overall, this site- and subtype-specific immune response is likely to play a role in the different biological behavior of DCIS subtypes.

Compliance with ethical standards

Conflict of interest The authors declare that they have no conflict of interest.

Publisher's note Springer Nature remains neutral with regard to jurisdictional claims in published maps and institutional affiliations.

References

1. Barnes NLP, Ooi JL, Yarnold JR, Bundred NJ. Ductal carcinoma in situ of the breast How does DCIS develop? BMJ. 2012;344:e797.
2. Bleyer A, Welch HG. Effect of three decades of screening mammography on breast-cancer incidence. N Engl J Med. 2012; 367:1998–2005.
3. Goldhirsch A, Winer EP, Coates AS, Gelber RD, Piccart-Gebhart M, Thürlimann B, et al. Personalizing the treatment of women with early breast cancer: highlights of the st gallen international expert consensus on the primary therapy of early breast Cancer 2013. Ann Oncol. 2013;24:2206–23.
4. Agahozo MC, Van Bockstal MR, Groenendijk FH, van den Bosch TPP, Westenend P, van Deurzen CHM. Ductal carcinoma in situ of the breast: immune cell composition according to subtype. Mod Pathol. 2020;33:196–205.
5. Doebar SC, van den Broek EC, Koppert LB, Jager A, Baaijens MHA, Obdeijn IMAM, et al. Extent of ductal carcinoma in situ according to breast cancer subtypes: a population-based cohort study. Breast Cancer Res Treat. 2016;158:179–87.
6. Agahozo MC, Hammerl D, Debets R, Kok M, van Deurzen CHM. Tumor-infiltrating lymphocytes and ductal carcinoma in situ of the breast: friends or foes? Mod Pathol. 2018;31:1012–25.
7. Van Bockstal M, Lambein K, Gevaert O, De Wever O, Praet M, Cocquyt V, et al. Stromal architecture and periductal decorin are potential prognostic markers for ipsilateral locoregional recurrence in ductal carcinoma in situ of the breast. Histopathology. 2013;63:520–33.
8. Pruneri G, Lazzeroni M, Bagnardi V, Tiburzio GB, Rotmensz N, DeCensi A et al. The prevalence and clinical relevance of tumor-infiltrating lymphocytes (TILs) in ductal carcinoma in situ of the breast. Ann Oncol. 2017;28:321–8.
9. Toss MS, Miligy I, Al-Kawaz A, Alsleem M, Khout H, Rida PC, et al. Prognostic significance of tumor-infiltrating lymphocytes in ductal carcinoma in situ of the breast. Mod Pathol. 2018;31:1226–36.
10. Dieci MV, Radosevic-Robin N, Fineberg S, Van Den Eynden G, Ternes N, Penault-Llorca F et al. Update on tumor-infiltrating lymphocytes (TILs) in breast cancer, including recommendations to assess TILs in residual disease after neoadjuvant therapy and in carcinoma in situ: a report of the International Immuno-Oncology Biomarker Working Group on Bre. Semin Cancer Biol. 2018;52:16–25.
11. Campbell MJ, Baehner F, O'Meara T, Ojukwu E, Han B, Mukhtar R, et al. Characterizing the immune microenvironment in high-risk ductal carcinoma in situ of the breast. Breast Cancer Res Treat. 2017;161:17–28.

12. Thompson E, Taube JM, Elwood H, Sharma R, Meeker A, Warzecha HN, et al. The immune microenvironment of breast ductal carcinoma in situ. Mod Pathol. 2016;29:249–58.

13. Wasserman JK, Parra-Herran C. Regressive change in high-grade ductal carcinoma in situ of the breast: histopathologic spectrum and biologic importance. Am J Clin Pathol. 2015;144:503–10.

14. Miligy I, Mohan P, Gaber A, Aleskandarany MA, Nolan CC, Diez-Rodriguez M, et al. Prognostic significance of tumour infiltrating B-lymphocytes in breast ductal carcinoma in situ. Histopathology. 2017;71:258–68.

15. Morita M, Yamaguchi R, Tanaka M, Tse GM, Yamaguchi M, Kanomata N, et al. CD8 + tumor-infiltrating lymphocytes contribute to spontaneous "healing" in HER2-positive ductal carcinoma in situ. Cancer Med. 2016;5:1–12.

16. Chivukula M, Domfeh A, Carter G, Tseng G, Dabbs DJ. Characterization of high-grade ductal carcinoma in situ with and without regressive changes: diagnostic and biologic implications. Appl Immunohistochem Mol Morphol. 2009;17:495–9.

17. Horii R, Akiyama F, Kasumi F, Koike M, Sakamoto G. Spontanious "healing" of breast cancer. Breast Cancer. 2005;12:140–4.

18. Dutch Institute for Clinical Auditing. Factsheet Indicatoren NABON Breast Cancer Audit (NBCA) 2017, Leiden, 2017 https://www.zorginzicht.nl/bibliotheek/Borstkanker/RegisterMeetinstrumenten Documenten/Indicatorgids. Accessed 19 Sep 2018.

19. Wolff AC, Hammond MEH, Hicks DG, Dowsett M, McShane LM, Allison KH et al. Recommendations for human epidermal growth factor receptor 2 testing in breast cancer: american society of clinical oncology/college of american pathologists clinical practice guideline update. Arch Pathol Lab Med. 2014.

20. FEDERA. Human Tissue and Medical Research: Code of conduct for responsible use (2011). Rotterdam, 2011 https://www.federa.org/sites/default/files/digital_version_first_part_code_of_conduct_in_uk_2011_12092012.pdf. Accessed 12 Sep 2018.

21. Mitchell E, Jindal S, Chan T, Narasimhan J, Sivagnanam S, Gray E et al. Loss of myoepithelial calponin-1 characterizes high-risk ductal carcinoma in situ cases, which are further stratified by T cell composition. Mol Carcinog. 2020. https://doi.org/10.1002/mc.23171.

22. Liu F, Lang R, Zhao J, Zhang X, Pringle GA, Fan Y, et al. CD8 + cytotoxic T cell and FOXP3 + regulatory T cell infiltration in relation to breast cancer survival and molecular subtypes. Breast Cancer Res Treat. 2011;130:645–55.

23. Bates GJ, Fox SB, Han C, Leek RD, Garcia JF, Harris AL, et al. Quantification of regulatory T cells enables the identification of high-risk breast cancer patients and those at risk of late relapse. J Clin Oncol. 2006;24:5373–80.

24. Mahmoud SM, Paish EC, Powe DG, Macmillan RD, Lee AH, Ellis IO, et al. An evaluation of the clinical significance of FOXP3+ infiltrating cells in human breast cancer. Breast Cancer Res Treat. 2011;127:99–108.

25. West NR, Kost SE, Martin SD, Milne K, Deleeuw RJ, Nelson BH, et al. Tumour-infiltrating FOXP3(+) lymphocytes are associated with cytotoxic immune responses and good clinical outcome in oestrogen receptor-negative breast cancer. Br J Cancer. 2013;108:155–62.

26. Bense RD, Sotiriou C, Piccart-Gebhart MJ, Haanen JBAG, van Vugt MATM, de Vries EGE. et al. Relevance of tumor-infiltrating immune cell composition and functionality for disease outcome in breast cancer. J Natl Cancer Inst. 2017;109:djw192

27. Akkari L, Sloane BF, Olson OC, Bos PD, Martinez LM, Robila V, et al. Regulatory T cells control the switch from in situ to invasive breast cancer. Front Immunol. 2019;10:1492.

28. Costa A, Kieffer Y, Scholer-Dahirel A, Pelon F, Bourachot B, Cardon M, et al. Fibroblast heterogeneity and immunosuppressive environment in human breast cancer. Cancer Cell. 2018;33:463–.e10.

29. Castle JC, Uduman M, Pabla S, Stein RB, Buell JS. Mutation-derived neoantigens for cancer immunotherapy. Front Immunol. 2019;10:1856.

30. Van Bockstal M, Libbrecht L, Floris G, Lambein K, Pinder S. Stromal inflammation, necrosis and HER2 overexpression in ductal carcinoma in situ of the breast: another causality dilemma? Ann Oncol. 2017;28:2317–2317.

31. Mohammed ZMA, Going JJ, Edwards J, Mcmillan DC. The role of the tumour inflammatory cell infiltrate in predicting recurrence and survival in patients with primary operable breast cancer. Cancer Treat Rev. 2012;38:943–55.

32. Dano H, Altinay S, Arnould L, Bletard N, Colpaert C, Dedeurwaerdere F, et al. Interobserver variability in upfront dichotomous histopathological assessment of ductal carcinoma in situ of the breast: the DCISion study. Mod Pathol. 2019;33:354–66.